

Correlations of chiral condensate and quark number densities with static quark sources

Kay Hübner^{*†}

Brookhaven National Lab, Upton, NY 11973

E-mail: huebner@bnl.gov

We investigate correlation functions of the Polyakov loop and static meson/diquark systems with the chiral condensate and the quark number density at finite temperature. In particular the latter observable can give insight into the mechanism of screening and string breaking at finite temperature. We use for our analysis gauge field configurations generated in 2+1 flavor QCD with an improved staggered fermion action with almost physical light quark masses and a physical value of the strange quark mass on lattices with temporal extent $N_\tau = 4$ and 6.

*The XXV International Symposium on Lattice Field Theory
July 30-4 August 2007
Regensburg, Germany*

^{*}Speaker.

[†]for the RBC-Bielefeld Collaboration, together with C. Schroeder, UC San Diego

1. Introduction

Global expectation values of the chiral condensate and quark number density give information about the structure of the thermal medium at finite temperature and non-zero chemical potential μ . Calculating these observables *locally*, i. e. depending on their spatial position, allows for a spatially resolved analysis of dynamical quark clouds and the chiral condensate density around static quark, diquark or Meson sources. We investigate correlation functions of the chiral condensate/quark number density with the Polyakov loop or products of Polyakov loops, which allow to probe the screening and string breaking mechanism of systems composed of static color charges at finite temperature. Lattice calculations of these operators have been performed in the past with staggered and Wilson quarks [1, 2, 3, 4] for rather large quark masses and on small lattices. The investigations presented here form the basis for future studies of the spatial correlators of the quark number density, which has been proposed as a means to decide whether the QGP has a liquid phase [5].

2. Operators

We have calculated the chiral condensate and the quark number density depending on their spatial position \mathbf{x} by using

$$\bar{\chi}\chi^f(\mathbf{x}) = \frac{n_f}{4N_\tau} \text{Tr}_c \sum_{x_0} \mathbf{M}_{f,xx}^{-1} \quad \text{and} \quad n_q^f(\mathbf{x}) = \frac{n_f}{4N_\tau} \text{Tr}_c \sum_{y,x_0} \mathbf{M}_{f,xy}^{-1} \frac{\partial \mathbf{M}_{f,xx}}{\partial \mu_f}, \quad (2.1)$$

where $x = (x_0, \mathbf{x})$, $f = 1, \dots, n_f$ labels the flavor, μ_f is the corresponding chemical potential and Tr_c denotes the trace in color space, with $\text{Tr}_c \mathbf{1} = 1$. Derivatives with respect to μ_f are evaluated at $\mu_f = 0$. We can now calculate the correlator of $\bar{\chi}\chi^f(\mathbf{x})$ and $n_q^f(\mathbf{x})$ with the Polyakov loop $L(\mathbf{x})$ or products of Polyakov loops, for which we use

$$L(\mathbf{x}) = Z(g^2)^{N_\tau} \text{Tr}_c \prod_{x_0=0}^{N_\tau-1} U_4(x_0, \mathbf{x}), \quad C_{Q\bar{Q}}(r) = L(0)L^*(r), \quad C_{QQ}(r) = L(0)L(r), \quad (2.2)$$

where L , and therefore also $C_{Q\bar{Q}}$ and C_{QQ} , is properly renormalised by the multiplicative renormalisation constant $Z(g^2)^{N_\tau}$, which is determined at $T = 0$ from a matching of the static quark potential to the string potential. The $C_{Q\bar{Q}}$ and C_{QQ} describe static meson and diquark systems, respectively. The correlation functions $\langle n_q^f(\mathbf{x})L(\mathbf{y}) \rangle$ and $\langle n_q^f(\mathbf{x})C_s(r) \rangle$ for $s = QQ, Q\bar{Q}$ are then properly renormalised as well. The renormalisation for $\bar{\chi}\chi^f$ involves both multiplicative and additive renormalisation constants. In order to eliminate the additive contributions, we calculate the *connected* correlator

$$\langle \bar{\chi}\chi^f(\mathbf{x})L(\mathbf{y}) \rangle_c = \langle \bar{\chi}\chi^f(\mathbf{x})L(\mathbf{y}) \rangle - \langle \bar{\chi}\chi^f \rangle \langle L \rangle, \quad (2.3)$$

which approaches the corresponding continuum expression $\langle \bar{\psi}\psi^f(\mathbf{x})L(\mathbf{y}) \rangle_c$ in the limit $a \rightarrow 0$.

In this work, we analyze gauge field configurations generated in 2+1 flavor QCD with the p4fat3 staggered fermion action, where the strange quark mass m_s is fixed to its physical value and the light quark mass is chosen as $m_l = 0.1m_s$. Lattice sizes are $16^3 \times 4, 6$ [6, 7]. For the calculation of expectation values we employed the random noise vector method with 100 random noise vectors.

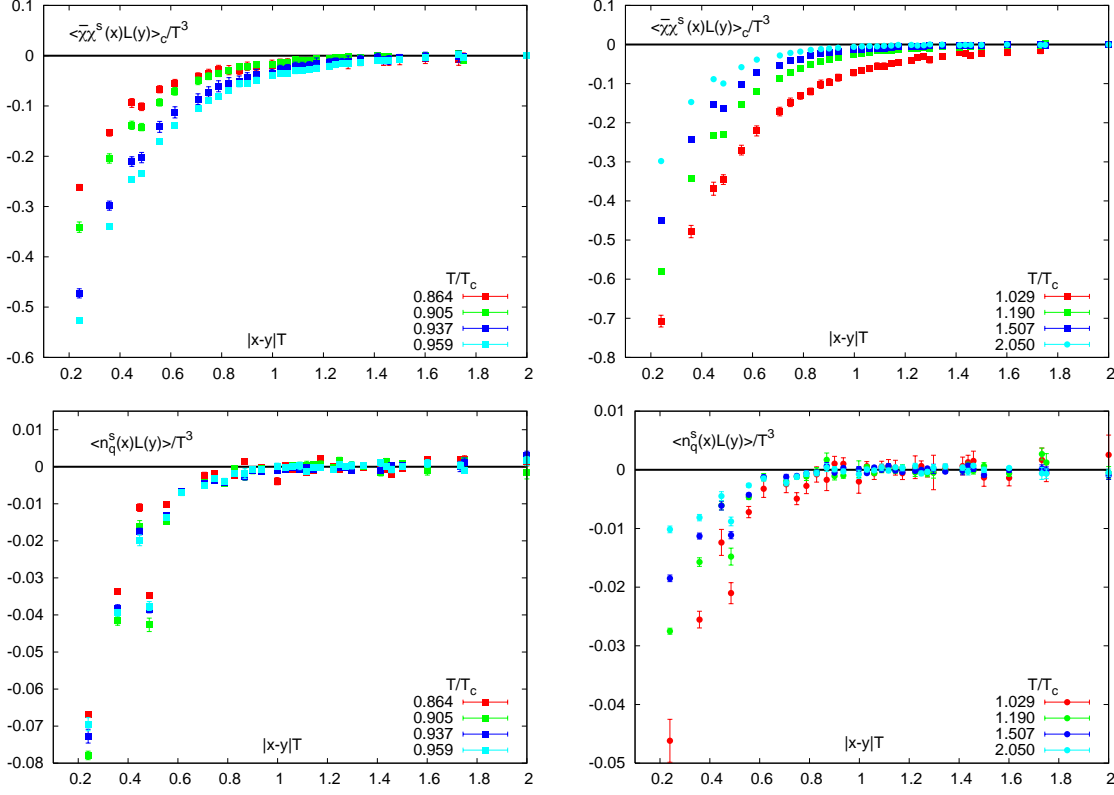


Figure 1: $\langle \bar{\chi} \chi^s L \rangle_c$ (upper row) and $\langle n_q^s L \rangle$ (lower row) for the strange quark species.

3. Results for $\langle \bar{\chi} \chi L \rangle_c$ and $\langle n_q L \rangle$

In fig. 1 we show the results for $\langle \bar{\chi} \chi^s L \rangle_c$ (upper row) and $\langle n_q^s L \rangle$ (lower row) for the strange quark species obtained from $N_\tau = 4$ lattices. We observe that all correlators vanish rapidly at distances $rT \gtrsim 1$, i. e. when $\bar{\chi} \chi^f$ and n_q^f approach their thermal expectation value undisturbed by the presence of the static quark. For small separations $\langle \bar{\chi} \chi^s L \rangle_c$ assumes smaller values, signalling a gradual restoration of chiral symmetry in the vicinity of the static quark. The correlator $\langle n_q^s L \rangle$ becomes smaller than zero for smaller separations as well, as the static quark source is screened by an excess of dynamical anti-quarks arranged in a cloud around the static quark. The effect becomes smaller above T_c , as thermal gluons are available in the deconfined phase to provide screening. All these findings are in qualitative agreement with those of earlier studies [1, 2, 3, 4].

For $\langle n_q^s L \rangle$ we observe a peculiar dip at $rT \approx 0.5$, which we investigate in more detail in fig. 2. Varying the lattice spacing, we see in fig. 2 (left), that the position of the dip varies with a as well, pointing at a lattice artifact that vanishes in the continuum limit. In fig. 2 (right) we computed $\langle n_q^s L \rangle$ at $T/T_c = 0.905, N_\tau = 4$ for p4, Naik and naive staggered discretisations of the fermion matrix \mathbf{M} . The artifact is present in all three discretisation schemes, thus its appearance is not dependent on the particular action used. Rather the mixing of different quantum channels in the staggered formulation is probably responsible for this effect.

In order to quantify further the behavior of these correlators, we have performed simple expo-

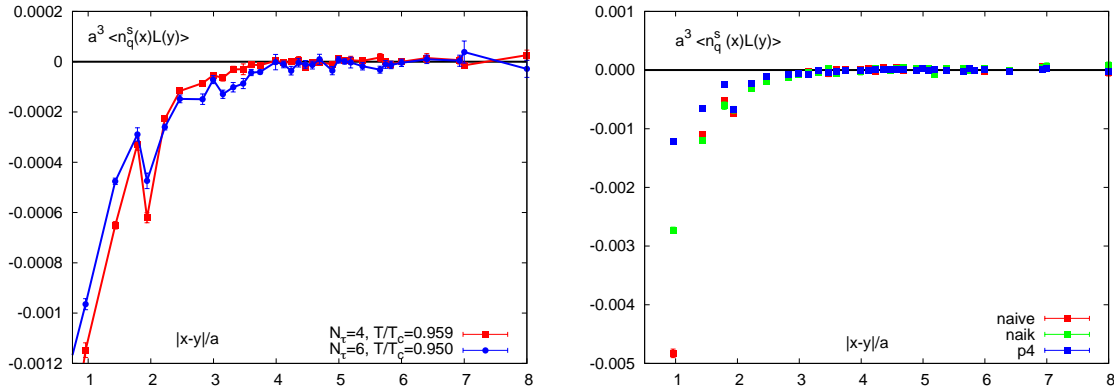


Figure 2: $\langle n_q^s \rangle$ for $N_\tau = 4$ and 6 (left) and for different staggered discretisations of the fermion matrix \mathbf{M} at $T/T_c = 0.905, N_\tau = 4$ (right).

ponential fits. The resulting screening masses $m^{l,s}$ of the correlator involving the chiral condensate density are, of course, not affected by the multiplicative renormalisation constants. In fig. 3 we show $\langle \bar{\chi}\chi^s L \rangle_c$ (upper row) and $\langle n_q^s L \rangle$ (lower row) for the strange quark species on a log-scale together with the results of the χ^2 -fits of exponential functions. We obtain similar results for the light quark species. The fit ranges employed were $0.3 \leq rT \leq 1$ for $\langle n_q^f L \rangle$, where we left out the values due to the artifact at $rT \approx 0.5$, and $0.1 \leq rT \leq 1.2$ for $\langle \bar{\chi}\chi^f L \rangle_c$.

The results for the screening masses obtained from the fits with exponential functions are shown in fig. 4(left). As expected¹ the screening masses obtained from $\langle n_q^f L \rangle$ are larger than those from $\langle \bar{\chi}\chi^f L \rangle_c$ and we generally find m^s is larger than m^l . We observe a drop of all screening masses close to T_c , as all correlation functions become large in the cross over region. For large temperatures we have $m^{l,s}/T \ll 1$ and we therefore expect $m^l = m^s$ to hold, which is not yet the case at $T/T_c = 2$. Moreover, the deviation of the data from the lattice with smaller aspect ratio points to volume effects which are still present in our calculations of $m^{l,s}$. The Debye masses extracted from the $N_\tau = 6$ lattices are roughly of the same size as the screening masses [9]. In order to avoid contamination from excited states, we plan to study $p = 0$ projections of the correlators in the future.

The total induced quark number of flavor f around a static anti-quark can be computed by

$$\langle N_q^f \rangle_{\bar{Q}} = \frac{\langle L^* \sum_{\mathbf{x}} n_q^f(\mathbf{x}) \rangle}{\langle \text{Re } L \rangle}, \quad (3.1)$$

where we show the results of our calculation in fig. 4(right). As was already observed in 2-flavor QCD [10], $\langle N_q^f \rangle_{\bar{Q}}$ vanishes rapidly for $T > T_c$, where screening is predominantly provided by thermal gluons. For $T \rightarrow 0$ the induced quark number approaches one, where this limit is approached faster for light quarks than the strange flavor, since the heavier sea quarks are more difficult to induce.

¹For heavy sea quarks the correlation functions $\langle \bar{\chi}\chi^f L \rangle_c$ and $\langle n_q^f L \rangle$ can be related to hopping parameter expansions of real and imaginary parts of Polyakov loops, respectively[2]. In this limit one finds at high temperatures $m_{n_q L}/m_{\bar{\chi}\chi L} = 1.5$ [8].

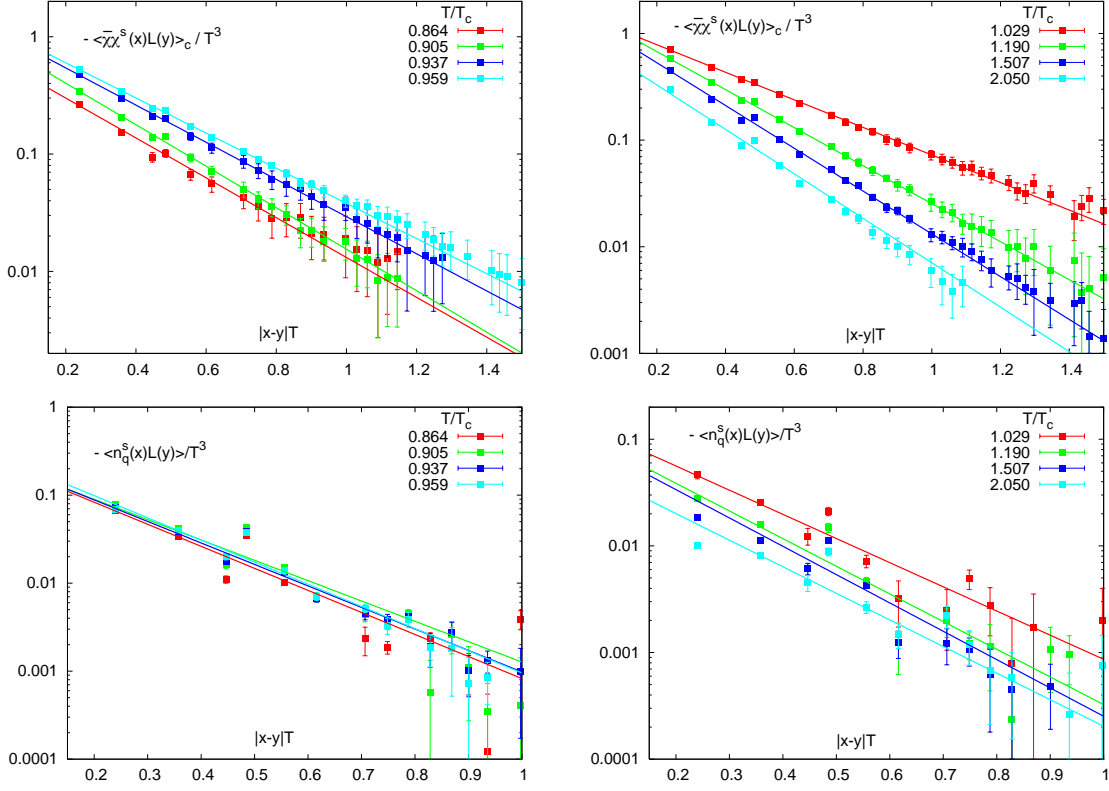


Figure 3: $\langle \bar{\chi}\chi^s L \rangle_c$ (upper row) and $\langle n_q^s L \rangle$ (lower row) for the strange quark species on a log-scale. Lines are the results of the χ^2 -fits with simple exponential functions.

4. Results for $\langle n_q C_{QQ} \rangle$ and $\langle n_q C_{Q\bar{Q}} \rangle$

We now turn to the computation of three point correlation functions $\langle n_q C_{QQ} \rangle$ and $\langle n_q C_{Q\bar{Q}} \rangle$. In fig. 5 we show $\langle n_q^s(\mathbf{x}_1, \mathbf{x}_2) C_{QQ}(r) \rangle$ for $T/T_c = 0.905$, calculated on lattices with temporal extent $N_\tau = 4$ for separations $rT = 1.25$ (left) and $rT = 0.25$ (right) of the Polyakov loops, which are placed at $\mathbf{x}_1 = \pm rT/2, \mathbf{x}_2 = 0$. We see that for large separations r the correlator assumes negative values centered around the individual positions of the static quarks. This signals an excess of dynamical anti-quarks and the screening mechanism is *mesonic*, i. e. $QQ \rightarrow Q\bar{q} + Q\bar{q}$, where Q stands for a static quark and q for a dynamical quark. For small separations we observe positive values of the correlator. Thus the screening mechanism has changed to *baryonic*, i. e. $QQ \rightarrow QQq$. This behavior has been observed in the induced quark number of the diquark system in 2-flavor QCD as well [10].

In fig. 6 we show the values of $\langle n_q^s C_{QQ} \rangle$ (left) and $\langle n_q^s C_{Q\bar{Q}} \rangle$ (right) along the line connecting the static quarks for several temperatures and two separations, where $\mathbf{x}_1 = x, \mathbf{x}_2 = 0$. The dotted lines mark the position of the Polyakov loops, where the anti-quark source in the $Q\bar{Q}$ -system is located at larger values of x . We see mesonic screening in the diquark system for large separations r at all T calculated here, whereas at the smallest distance only the lowest temperature turns to baryonic screening. In the $Q\bar{Q}$ -system the screening mechanism is mesonic for all T and rT , i. e. $Q\bar{Q} \rightarrow Q\bar{q} + \bar{Q}q$.

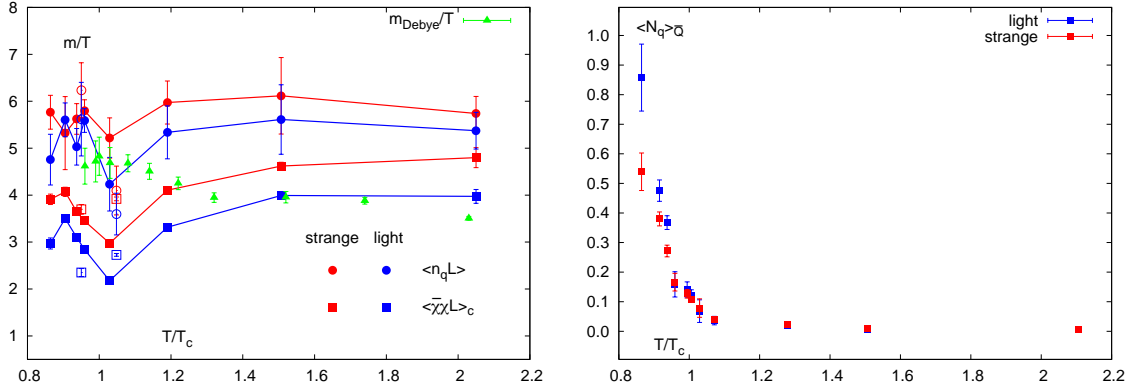


Figure 4: Left: Screening masses obtained from an exponential fit. Closed symbols: $N_\tau = 4$, open symbols: $N_\tau = 6$. Debye masses are taken from [9]. Right: Induced quark number around a static anti-quark.

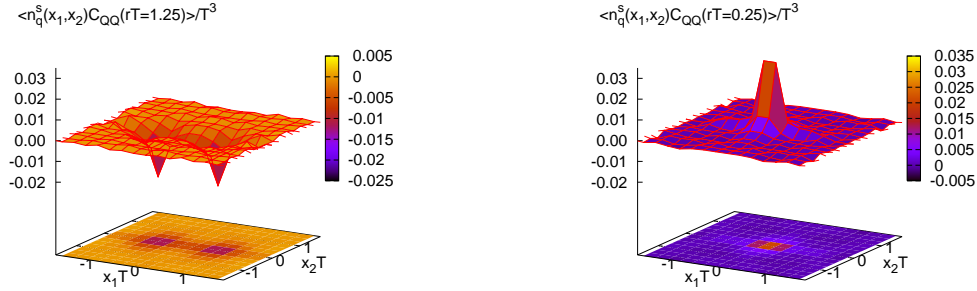


Figure 5: $\langle n_q^s C_{QQ} \rangle$ for $T/T_c = 0.905, N_\tau = 4$ at separations $rT = 1.25$ (left) and $rT = 0.25$ (right) of the Polyakov loops.

5. Conclusion and Outlook

We have studied correlators of the local chiral condensate density and the local quark number density with Polyakov loops in 2+1 flavor QCD with almost realistic quark masses at finite temperature on $16^3 \times 4, 6$ lattices. We found that the correlator of the Polyakov loop with the quark number density and the connected correlator with the chiral condensate density are well described by an exponential fit-Ansatz. We calculated the screening masses from these correlators and the induced quark number in the static quark system. Moreover, we investigated the quark number density in static diquark and mesonic systems, where we found the screening mechanism in the diquark system to change from mesonic to baryonic at small separations for small temperatures.

In the future we want to study the $p = 0$ projection of the correlators with the Polyakov loop to avoid contamination from excited states in the screening masses. Furthermore we like to examine lattices with a larger physical volume in order to get better control over finite volume effects. This work forms the basis for future computations of spatial correlators of the quark number density $\langle n_q(0)n_q(r) \rangle$, which might shed light on whether the QGP has a liquid phase [5].

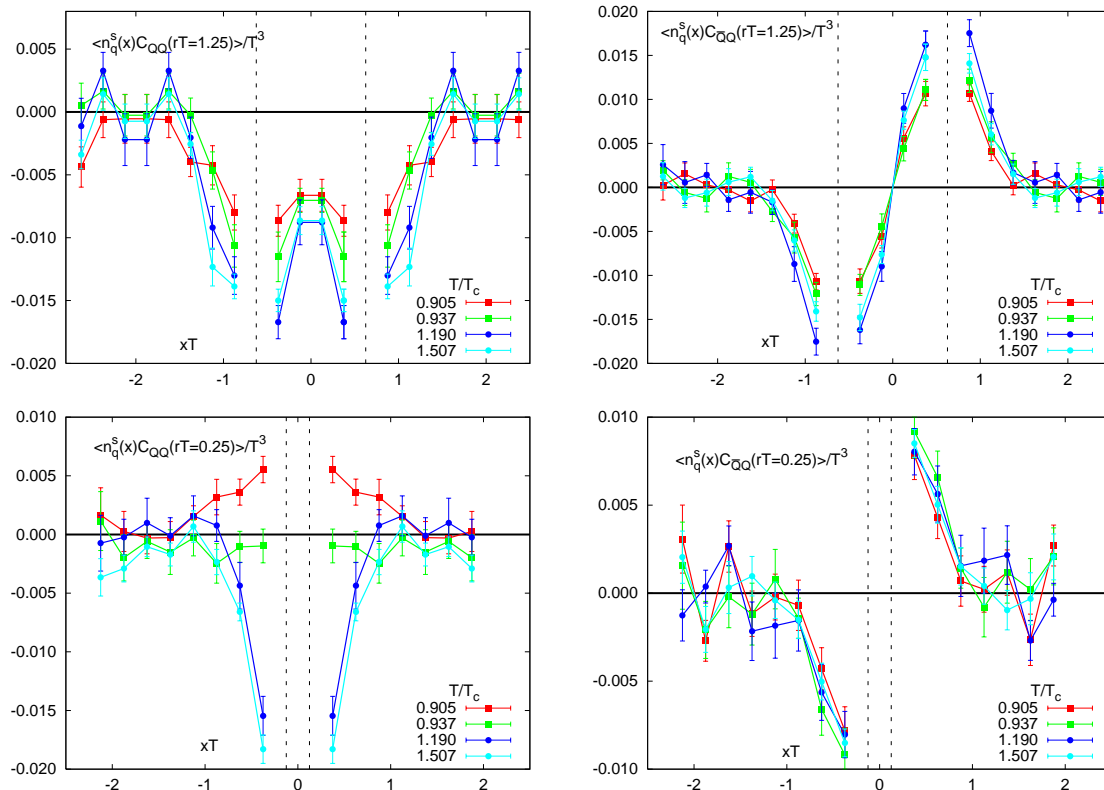


Figure 6: Cut along the connecting axis of the static quarks, $\langle n_q^s C_{QQ} \rangle$ (left) and $\langle n_q^s C_{\bar{Q}\bar{Q}} \rangle$ (right) for several temperatures. The dotted lines give the position of the Polyakov loops.

6. Acknowledgement

This manuscript has been authored under contract number DE-AC02-98CH10886 with the U. S. Department of Energy.

References

- [1] W. Feilmair, M. Faber and H. Markum, *Phys. Lett. B* **221** (1989) 363.
- [2] W. Feilmair, M. Faber and H. Markum, *Phys. Rev. D* **39** (1989) 1409.
- [3] W. Sakuler *et al.*, *Phys. Lett. B* **276** (1992) 155.
- [4] W. Buerger, M. Faber, H. Markum, M. Muller and M. Schaler, *Nucl. Phys. Proc. Suppl.* **34** (1994) 269.
- [5] M. H. Thoma, *Nucl. Phys. A* **774** (2006) 307.
- [6] Jan van der Heide, these proceedings, PoS(LATTICE 2007) 234.
- [7] M. Cheng *et al.*, *Phys. Rev. D* **74** (2006) 054507.
- [8] S. Nadkarni, *Phys. Rev. D* **33** (1986) 3738.
- [9] K. Petrov, these proceedings, PoS(LATTICE 2007) 217.
- [10] M. Doring, K. Hubner, O. Kaczmarek and F. Karsch, *Phys. Rev. D* **75** (2007) 054504.